31st Annual International Conference of the IEEE EMBS
Minneapolis, Minnesota, USA, September 2-6, 2009

Developing a Hybrid Computational Model of AFM Indentation for Analysis of Mechanically Heterogeneous Samples

Evren U. Azeloglu, Gaurav Kaushik and Kevin D. Costa

Abstract — **Standard analysis methods for atomic force microscope (AFM) indentation experiments use Hertzian contact mechanics to extract local elastic properties assuming a homogeneous sample material. In contrast, most biological materials have heterogeneous structure and composition. We previously introduced a non-Hertzian analysis method to detect depth-dependent elastic properties from indentation depth, force and geometry information. In this study we employ a modified Eshelby model to characterize the elastic properties of heterogeneous substrates with discrete embedded inclusions. In this hybrid computational model, we estimate the contribution of inclusions with known size and moduli to the overall indentation response of a heterogeneous substrate based on the effective volume fraction of constituents within the indentation field. For wide ranges of indenter size and inclusion geometry, simulations reveal a consistent ellipsoidal indentation field, suggesting the Eshelby model may be applicable for large discrete inclusions. This novel technique provides a potential means to calculate inclusion properties of heterogeneous materials, such as cells and tissues, using AFM indentation without physical deconstruction of the composite sample.**

I. Introduction

MULTISCALE modeling of complex biomechanical systems requires accurate knowledge of microscopic elastic properties of the key constituents. Most microscale mechanical measurement techniques operate under simplifying assumptions such as isotropic linear elasticity, and homogeneity of the sample. In contrast, cells and tissues have complex mechanical properties often coupled with heterogeneities in structure and composition. Such heterogeneity plays a critical role in determining how physical forces are transferred to the mechanosensitive protein machinery within the cell [1]. Intuitively, different components of an inhomogeneous material are expected to respond differently under mechanical loading; thus, internal organelles and other cytoskeletal and extracellular components can have a significant effect on the distribution of mechanical stress.

A common goal of biomechanical studies is to gain insight into the structural workings of the tissue of interest such that the importance of individual components and their biological or biophysical roles in health and disease can be realized [2]. Computational modeling of tissue properties is critical to understand such mechanobiological relationships. For example, by histologically deconstructing the underlying laminar architecture of the myocardium and mathematically transforming local kinematic measures using a microstructural basis, new insights into the mechanism of ventricular contraction have been obtained [3, 4]. Phenomenological material models, on the other hand, operate on a different premise. While they may succeed in mimicking the mechanical behavior of tissue under deformation -- such as biaxial properties of the aortic wall [5] -- they are not intended to elucidate the underlying biophysical relationships. Herein, we introduce a hybrid method that involves both structural modeling using finite element analysis and phenomenological modeling based on elastic homogenization theory, with the objective of enhancing AFM indentation testing as a reliable means to characterize multi-component biological substrates for multiscale biomechanics applications.

II. Materials and Methods

A. Theory

Eshelby's homogenization theory estimates the equilibrium effective elastic properties of heterogeneous materials with sparse, uniformly distributed spherical inclusions, given the volume fraction of the constituents [6]. Recent studies have successfully extended its applicability to higher volume ratios [7]. Accordingly, the effective elastic constants, K and μ, for a given heterogeneous material with known substrate (M) and inclusion (Ω) properties can be determined using the following equations:

$$K_{eff} = \left[1 - f_\Omega \left(\frac{K_M}{K_M - K_\Omega} - s_1\right)^{-1}\right] K_M \quad (1)$$

$$\mu_{eff} = \left[1 - f_\Omega \left(\frac{\mu_M}{\mu_M - \mu_\Omega} - s_2\right)^{-1}\right] \mu_M \quad (2)$$

where f_Ω is the volume ratio of the inclusion, and s_1 and s_2 are components of the Eshelby tensor for an inclusion geometry of circular cross-section [7].

When the results of this modified Eshelby homogenization routine were compared to those reported by others in the literature [8], excellent agreement between the two models was observed (data not shown).

Manuscript received April 23, 2009. This work was supported in part by the National Science Foundation CAREER Award BES-0239138.

EUA (evren.azeloglu@mssm.edu) and KDC (kevin.costa@mssm.edu) were formerly with the Department of Biomedical Engineering at Columbia University. They are now with the Cardiovascular Research Center in the Department of Medicine (Cardiology) at Mount Sinai School of Medicine, New York, NY 10029 USA (phone: 212-241-7122; fax: 212-241-4080).

GK (gk2218@columbia.edu) is with the Department of Biomedical Engineering at Columbia University.

B. Finite Element Modeling

To test the applicability of analytical homogenization to AFM indentation experiments, computational studies were performed in which the indentation response was computed for idealized inhomogeneities introduced into an isotropic elastic substrate.

A finite element model (FEM) simulation of AFM indentation was developed in ABAQUS Standard (v6.7; Simulia, Providence, RI) similar to our previously reported approach [9]. A thick, isotropic, linear elastic cylindrical substrate of 50-μm height and 50-μm radius was bound at its bottom axial (z-plane) surface with frictionless constraints allowing radial expansion. A large substrate indentation depth of 3 μm was selected to mimic testing of larger tissue samples to be investigated in later stages of this work. For some of the heterogeneity conditions, Abaqus Explicit was used since it reached convergence at greater indentation depths compared to Abaqus Standard.

The substrate was meshed with 10,000 structured 4-node linear continuum axisymmetric elements with reduced integration (CAX4R). A meshing bias of 10X toward the top center of the mesh was introduced in both radial and axial directions to accommodate kinematic nonlinearities in the immediate vicinity of the indentation site. In addition, arbitrary Lagrangian-Eulerian mesh adaptivity was employed for smaller indenter geometries at a frequency ranging from 1-20 increments with 2-10 remeshing sweeps, iteratively applied to avoid excessive distortion of the mesh under large local deformations.

The indenter was modeled as an analytical rigid spherical surface coming into hard (direct) surface-to-surface contact with the substrate, with maximum contact clearance of 0.2 μm. A no-slip friction condition was enforced at the interface, although frictionless and low-friction indentations were also tested for homogeneous substrate conditions in order to evaluate associated effects on the results. Even though it was theoretically redundant, the indenter had to be further constrained along the indentation axis against moments; failure to provide this constraint caused clearly inaccurate deformations. The simulation started with the indenter at a resting position on the substrate surface (radial, axial = 0, 0), and a 3-μm axial displacement (indentation) was prescribed as a time-independent (static, general) step with a minimum of 20 increments.

Simulations were performed on a 2.0 GHz Intel Core Duo processor personal computer (Apple Computer, Cupertino, CA) with 2 GB of memory (at least 512 MB reserved for operation), and they typically ran for 60 seconds with values ranging from 15 to 330 seconds depending on the indenter size, substrate heterogeneity and adaptivity settings. Three different material heterogeneity conditions were tested as well as four different spherical indenter sizes. The heterogeneity conditions were either a horizontal 3-μm thick layer, a vertical 3-μm radius column, or an embedded 2-μm diameter sphere, respectively named *layer*, *column* and *zone* conditions. These conditions were chosen as simplified cases to gain an understanding of the complexities of testing composite materials, and not to represent particular biological samples. The indenters were 5 μm (*zone* only), 10 μm (*layer*, *column*, *zone*), 15 μm (*layer*, *column*) and 25 μm (*layer*, *column*) diameter spheres representing a range commonly used in AFM nanoindentation studies. Even though only linear elastic materials were tested, a variety of stiffness combinations yielded a wide range of indentation responses. For the *layer* and *column* conditions, inclusions that were stiffer than the surrounding matrix were employed whereas for the spherical *zone* condition, both soft and stiff inclusions were tested. It should also be noted that the *zone* condition used an advancing-front algorithm with quad-dominated free elements to mesh the sample due to inapplicability of structured elements with the round shape of the inclusion.

After a simulation was completed, the net reaction force on the indenter, F_{FEM}, and the indentation depth, h, were extracted at each incremental load step for post-processing. The pointwise apparent elastic modulus, $\hat{E}_{\mathrm{pw}}$, was then computed according to:

$$\hat{E}_{\mathrm{pw}} = \frac{3}{8}\frac{F_{\mathrm{FEM}}}{\sqrt{Rh^3}} \tag{3}$$

where R is the indenter radius [9]. $\hat{E}_{\mathrm{pw}}$ can easily be related to the Young's modulus, E_Y, of an equivalent elastic substrate via:

$$\hat{E}_{\mathrm{pw}} = \frac{E_Y}{2\left(1-\upsilon^2\right)} = \frac{9\mu_{eff}K_{eff}}{2(1-\upsilon^2)(\mu_{eff}+3K_{eff})} \tag{4}$$

where ν is Poisson's ratio, with μ_{eff} and K_{eff} defined above. Material incompressibility (ν = 0.5) was assumed for all simulations in this study.

C. Hybrid Modeling

Results from the finite element analysis using Equation (3) were combined with the modified homogenization theory using Equations (1) and (2) and the known material properties of the inclusion and substrate. This process led to a theoretical estimate of the corresponding volumetric contributions of the inclusion and the surrounding substrate to the overall effective apparent modulus as a function of indentation depth.

III. Results and Discussion

A. Depth-Dependent Pointwise Modulus

All FEM simulated heterogeneity conditions produced non-linear depth-dependent changes in pointwise apparent modulus. Both the *layer* and *column* scenarios produced logarithmically decaying effective moduli (**Figure 1A**), whereas the spherical *zone* inclusion problem resulted in a slight initial increase followed by a logarithmic decay (**Figure 2**). These results suggested that the stiffening effect of inclusions -- regardless of their geometric shape and position -- was reduced as the field of indentation grew with the increasing indentation depth. Under the *zone* condition, due to the large indentation field, no significant increase in effective modulus was observed at depths greater than 2 μm. Friction had little effect to the overall indentation response.

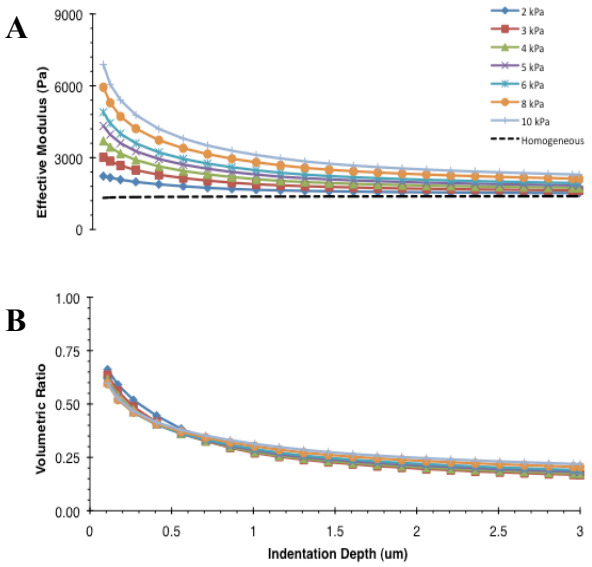

Figure 1. (A) Depth-dependent pointwise apparent modulus from representative *column* condition using 25-µm indenter with inclusions ranging from 1 to 20 kPa in a bulk material of 1 kPa. **(B)** The associated family of curves for the calculated inclusion volume ratio according to Eshelby homogenization theory (solved with Abaqus Standard).

The resultant modulus essentially represented the *effective apparent modulus* of the composite, which was used with Eshelby's homogenization theory to back-calculate the equivalent volume ratio of the inclusion knowing the prescribed inclusion and matrix moduli. Accordingly, the computed family of volume ratio curves for the representative *layer* case in **Figure 1A**, with 1 kPa bulk material and a range of inclusion moduli, is shown in **Figure 1B**. Similar results were found for the *column* and *zone* cases, indicating that the relative size of the inclusion diminishes as the indentation depth increases due to the expanding indentation field.

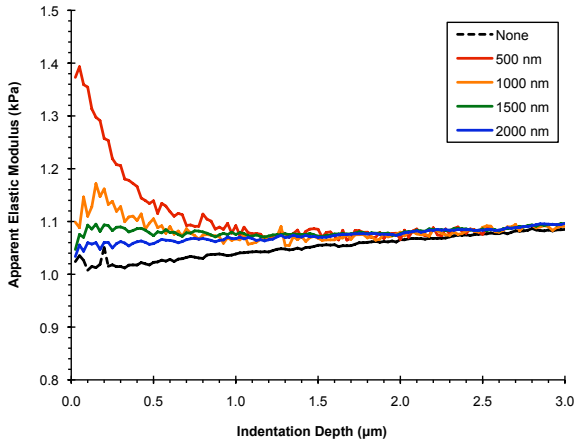

Figure 2. Effect of inclusion location on the effective elastic modulus for the *zone* condition in which the depth of the 2 µm spherical inclusion is shifted. Legend indicates distance between substrate surface and top of inclusion; "None" refers to the homogeneous case with no inclusion (solved with Abaqus Explicit).

B. Universal Indentation Field

Noting the similarity in the resultant volumetric ratio curves, despite the 20-fold range of inclusion moduli, it was hypothesized that a universal mathematical relationship might govern the *indentation field*, insensitive to the elastic properties of the heterogeneities for the three configurations tested in this study. To test this hypothesis an ellipsoid geometry was fitted by least-squares minimization to the combined *layer* and *column* cases, such that the relative volume of the inclusion within the indentation field matched the theoretical volume ratio under both scenarios; this concept is visually represented in **Figure 3** for the *layer* condition. The fitting procedure revealed that the axial extent of the indentation field was approximately 5.3 times the depth of indentation. This value was close to the empirical zero-stress border (values less than 5% of the maximum compressive stress) observed in FEM simulations of uniform homogeneous substrates, which occurred at 4.7 times the indentation depth. Same border for the *zone* condition occurred at around 4.1 times the depth. As a consequence of this large indentation field, it became prohibitively difficult to detect deep inclusions of finite size as demonstrated by the diminishing effect of the inclusion illustrated in **Figure 2**. In addition, small inclusions relative to the indentation field were difficult to detect irrespective of the inclusion modulus (data not shown).

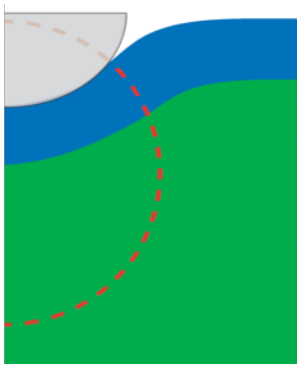

Figure 3. Axisymmetric view of hypothesized universal ellipsoidal *indentation field* (red curve) that occupies both the substrate (*green*) and the inclusion (*blue*).

C. Limitations

The method developed herein currently applies to heterogeneous substrates made up of isotropic linear elastic materials only. However, it can be extended to nonlinear or anisotropic materials by adjusting the components of the Eshelby tensor in Equations (1) and (2). Since the current finite element analysis was carried out on an axisymmetric domain, the results would apply only to symmetrical problems. Future studies will focus on developing more realistic 3-D simulations with non-collinear heterogeneities.

IV. Conclusion

This proof-of-concept modeling study demonstrates how the effective homogenized material properties obtained from AFM indentation experiments can be computationally deconstructed to obtain knowledge of inclusion geometry and/or material properties. The simulations revealed an ellipsoidal indentation field that extends approximately 4X to 5X of the indentation depth. Accordingly, finite sized heterogeneities that are located deeper than a small

proportion of the indenter radius would not be expected to significantly alter the force-depth response in AFM experiments. We have observed that the size of the inclusion relative to the indentation field was more critical than its modulus for deconstruction of material properties.

These findings may assist in the rational design of AFM experiments in which parameters such as indenter diameter, maximum indentation depth, or spacing between indentations can be optimized for a given heterogeneous sample. The hybrid computational approach employed in this study is designed to be generally applicable to heterogeneous substrate systems including biological cells and tissues with measurable inclusion sizes (e.g. the cell nucleus), such that knowing the size and geometry of the inclusions, one can back-calculate the inclusion and substrate moduli without the need for physical or chemical dissociation of the constituents. Characterization of depth-dependent effects of subsurface heterogeneities can yield an improved understanding of material nonlinearities observed in a number of biological samples. In future studies, the depth-dependent pointwise apparent modulus will be combined with finite element models in an inverse fitting procedure to extract constituent material properties from AFM indentation experiments on such heterogeneous samples, starting with composite hydrogel phantoms designed specifically for model validation.

ACKNOWLEDGMENTS

The authors acknowledge Glenn C. Gomes and Evan T. Kao for technical assistance.

REFERENCES

[1] J. Lammerding, P.C. Schulze, T. Takahashi, S. Kozlov, T. Sullivan, R.D. Kamm, C.L. Stewart, and R.T. Lee, "Lamin A/C deficiency causes defective nuclear mechanics and mechanotransduction," *J Clin Invest*, vol. 113, (no. 3), pp. 370-8, Feb 2004.

[2] Y.C. Fung, *Biomechanics : Mechanical Properties of Living Tissues*, New York: Springer-Verlag, 1993.

[3] T.P. Usyk, J.H. Omens, and A.D. McCulloch, "Regional septal dysfunction in a three-dimensional computational model of focal myofiber disarray," *Am J Physiol Heart Circ Physiol*, vol. 281, (no. 2), pp. H506-14, Aug 2001.

[4] K.D. Costa, Y. Takayama, A.D. McCulloch, and J.W. Covell, "Laminar fiber architecture and three-dimensional systolic mechanics in canine ventricular myocardium," *Am J Physiol*, vol. 276, (no. 2 Pt 2), pp. H595-607, Feb 1999.

[5] A. Pandit, X. Lu, C. Wang, and G.S. Kassab, "Biaxial elastic material properties of porcine coronary media and adventitia," *Am J Physiol Heart Circ Physiol*, vol. 288, (no. 6), pp. H2581-7, Jun 2005.

[6] J.D. Eshelby, "The determination of the elastic field of an ellipsoidal inclusion, and related problems," *Proc R Soc A*, vol. 241, (no. 1226), pp. 376-396, 1957.

[7] S. Li, R. Sauer, and G. Wang, "A circular inclusion in a finite domain I. The Dirichlet-Eshelby problem," *Acta Mechanica*, vol. 179, (no. 1-2), pp. 67-90, 2005.

[8] Z. Hashin and S. Shtrikman, "A variational approach to the theory of the elastic behaviour of multiphase materials," *J Mech Phys Solids*, vol. 11, (no. 2), pp. 127-140, 1963.

[9] K.D. Costa and F.C. Yin, "Analysis of indentation: implications for measuring mechanical properties with atomic force microscopy," *J Biomech Eng*, vol. 121, (no. 5), pp. 462-71, Oct 1999.